

# **Extending the Total Neutron Emission Rate of Steady-state Deuterium Large Helical Plasma**

## **Guided by a Data-driven Approach**

Kunihiro Ogawa<sup>a,b</sup>, Mitsutaka Isobe<sup>a,b</sup>, and Masayuki Yokoyama<sup>a,b</sup>

<sup>a</sup>National Institute for Fusion Science, National Institutes of Natural Sciences, Toki, 509-5292, Japan

<sup>b</sup>The Graduate University for Advanced Studies, SOKENDAI, Toki, 509-5292, Japan

### **Abstract**

A trial for extending the total neutron emission rate ( $S_n$ ) was performed in the Large Helical Device (LHD) deuterium plasma experiment using a gas puff in order to show the way to realize a steady-state fusion reactor. In the 22nd experimental campaign of the LHD, a high  $S_n$  discharge was performed by the experimental scenario guided by a data-driven approach. A regression analysis of  $S_n$  was conducted beforehand using the externally controllable parameters based on the database of the previous three campaigns. Then, the high  $S_n$  record was successfully updated to be  $3.7 \times 10^{15}$  n/s in a steady-state discharge during the 22nd campaign in line with the regression expression. This study demonstrates that such a data-driven approach is effective for the gradual extension of  $S_n$  beyond the employed database.

Keywords: LHD, Deuterium experiment, Total neutron emission rate, data-driven approach, steady-

state plasmas

## 1. Introduction

The development of high-performance plasmas has been focused on currently running fusion plasma experiments to show the way toward a fusion reactor. There are a variety of plasma parameters, such as the ion temperature, the triple product, the plasma beta, and the fusion output. The fusion output is one of the most critical parameters in evaluating the reach toward a fusion burning plasma because electrical power will be generated by the energy of deuterium-tritium fusion neutrons absorbed by the blanket modules. At the same time, a method of controlling the fusion performance technique should be developed to control the energy output from a fusion reactor. In previous deuterium experiments performed in large tokamaks, a total neutron emission rate ( $S_n$ ) of over  $5 \times 10^{16}$  n/s was achieved [1-3]. For  $S_n$  prediction, empirical formula techniques were introduced in JET in order to adjust the aperture to avoid the saturation of the pulse counting rate in the neutron cameras in advance of discharges [4]. For helical devices, which have the advantage of steady-state operation over tokamaks, the performance of a fusion plasma in a relatively large-sized machine has been investigated in the Large Helical Device (LHD) [5] and Wendelstein 7-X [6]. The deuterium experiment in LHD was initiated in 2017 [7]. In the deuterium operation of LHD, the neutron emission from the so-called beam-thermal reaction is dominant [8, 9]. Therefore, by using comprehensive

neutron diagnostics, studies of beam ion confinement are advanced in LHD [10-23].

Investigation of  $S_n$  dependence on the magnetic configuration and the plasma density has been performed in the deuterium operation in LHD [10, 11]. It was found that a relatively high  $S_n$  is obtained in the vacuum magnetic axis position ( $R_{ax}$ ) of 3.55 m, the toroidal magnetic field strength ( $B_t$ ) of 2.89 T, and the line-averaged electron density ( $n_{e\_avg}$ ) of  $2 \times 10^{19} \text{m}^{-3}$  to  $3 \times 10^{19} \text{m}^{-3}$  [11, 24, 25]. For a high  $S_n$  discharge, the record of  $S_n$  in steady-state discharge using a gas puff was found to be  $\sim 3.1 \times 10^{15}$  n/s in the 19th campaign of the LHD experiment, which was the LHD's first deuterium campaign that used intensive electron cyclotron heating (ECH) and neutral beam (NB) injections. In the 22nd LHD campaign performed in FY2020, the guidance deduces because the data-driven approach was applied to consider a high  $S_n$  discharge scenario. Here, the data-driven approach is classified into a complementary method of the physics-based approach without physics considerations. The regression analysis for  $S_n$  values, which used the externally controllable parameters obtained during the 19th and 21st LHD campaigns, such as the line-averaged electron density and injection power of NB injections, was utilized to inspect the importance of each controllable parameter for achieving a high  $S_n$  [26] before starting 22nd campaign. This was the same approach used to obtain the regression expression for the thermal diffusivities in LHD [27]. This approach may be appropriate for controlling the fusion output in a fusion reactor in the future. This paper represents the extension of high  $S_n$  in LHD, guided by a regression approach.

## 2. Regression approach for the evaluation of parameter importance

High  $S_n$  discharge was performed using the full power heating of ECH, a negative ion-based neutral beam (N-NB), and a positive ion-based neutral beam (P-NB) during the 19th and 21st campaigns of the LHD experiment. In this regression analysis, the experimental data points satisfying the following general restrictions were sampled. (1) The experiment was conducted in the best magnetic configuration for high  $S_n$  that is  $B_t$  of 2.89 T, and  $R_{ax}$  of 3.55 m. (2) A discharge was performed using a deuterium gas puff. (3) Both N-NB and P-NB were injected deuterium beam without a breakdown or an unintended stop. (4) Plasma was deuterium dominant, e.g., the ratio of  $D\alpha$  to  $H\alpha$  intensities measured by visible spectroscopy [28] was above 90%. (5) To avoid the period of weak NB absorption, the timing is after 500 ms from the plasma initiation. Figure 1 shows the density dependence of  $S_n$  obtained during the 19th and 21st LHD campaigns. Here,  $S_n$  was measured using the neutron flux monitor [29, 30], and  $n_{e\_avg}$  was measured by a far-infrared interferometer [31]. Datasets were created at each timing for Thomson scattering diagnostics [32], that is, at intervals of 33 ms. The envelope of  $S_n$  shows that there is a peak of  $S_n$  at  $n_{e\_avg}$  of  $2 \times 10^{19}$ - $3 \times 10^{19} \text{ m}^{-3}$ . The steep increase of  $S_n$  in the relatively low  $n_{e\_avg}$  range is due to the improvement of beam-ion deposition, and the gradual decrease of  $S_n$  in the relatively high  $n_{e\_avg}$  region is due to the decrease of the electron temperature, which induces low beam-ion density because of the shorter slowing-down time [9, 11]. For the

regression analysis, the range of  $n_{e\_avg}$  of  $1 \times 10^{19}$ - $3 \times 10^{19} \text{ m}^{-3}$ , where the promising region of updating high  $S_n$  in steady-state discharge, was selected. Here, in this dataset, the injection power ranges of N-NB ( $P_{N-NB}$ ), P-NB ( $P_{P-NB}$ ), and ECH ( $P_{ECH}$ ) were 1.3 MW to 6 MW, 1.9 MW to 19 MW, and 1.0 MW to 3.8 MW, respectively. The total number of data points was 1590 from 443 available discharges. The regression analysis of  $S_n$  using only externally controllable parameters, e.g.,  $n_{e\_avg}$  [ $10^{19}\text{m}^{-3}$ ],  $P_{N-NB}$  [MW],  $P_{P-NB}$  [MW], and  $P_{ECH}$  [MW], were conducted to identify the critical parameters for achieving high  $S_n$ . To find the regression expression, a log-linear multivariate regression was performed. The preliminary regression analysis shows  $S_n = 10^{14.25} \times n_{e\_avg}^{0.50} \times P_{N-NB}^{0.73} \times P_{P-NB}^{0.35} \times P_{ECH}^{-0.07}$  with the coefficient of determination ( $R^2$ ) of 0.70. For considering experimental scenarios by using a relatively small number of parameters and acquisition of better  $R^2$ ,  $P_{ECH}$  was excluded from the regression analysis because of the relatively low importance of  $P_{ECH}$  compared with the other three parameters. The obtained regression expression  $S_n = 10^{14.25} \times n_{e\_avg}^{0.52} \times P_{N-NB}^{0.69} \times P_{P-NB}^{0.37}$  shows that  $P_{N-NB}$  has the largest exponent to an increase in  $S_n$ . Here,  $R^2$  reaches 0.84 [26]. The reason for the highest exponent in  $P_{N-NB}$  is that N-NB injects with relatively high energy up to 180 keV [33]. Here, the experimentally obtained  $S_n$  was 13% larger than the  $S_n$  predicted by the regression expression for the highest  $S_n$  point.

### 3. Update of high $S_n$ record in steady-state discharge guided by regression analysis

High  $S_n$  discharge in the 22nd LHD campaign was performed using ECH and the ion

cyclotron range of frequency heating (ICH), N-NB, and P-NB. Table 1 shows the comparison of maximum  $P_{\text{N-NB}}$  and  $P_{\text{P-NB}}$  during the 19th and 21st campaigns and in the 22nd campaign. In particular,  $P_{\text{N-NB}}$  increases significantly in the 22nd campaign from the previous campaigns. Here, by considering the improvements of  $P_{\text{N-NB}}$  and  $P_{\text{P-NB}}$ , the expected increase of  $S_n$  in the 22nd campaign from the previous campaigns using the regression formula is approximately 10%. Figure 2 shows the waveform of the new  $S_n$  record discharge using a deuterium gas puff. In this discharge,  $P_{\text{ECH}}$ , the injection power of ICH,  $P_{\text{N-NB}}$ , and  $P_{\text{P-NB}}$  increased up to 4.3 MW, up to 2.4 MW, 6.9 MW, and 19.3 MW, respectively. The central electron temperature ( $T_{e0}$ ) measured by Thomson scattering diagnostics and  $n_{e\_avg}$  at  $t \sim 5$  s were 5.5 keV and  $2.3 \times 10^{19} \text{ m}^{-3}$ , respectively. The time evolution of  $S_n$  shows that  $S_n$  gradually increased according to the injections of ECH, ICH, and N-NB from the beginning of the discharge and then substantially increased at  $t = 4.8$  s due to P-NB injections. The highest  $S_n$  with  $3.7 \times 10^{15} \text{ n/s}$  was successfully achieved at  $t = 5.236$  s. Therefore,  $S_n$  increased by approximately 20% compared with  $S_n$  achieved in the previous experiment.

The experimentally obtained  $S_n$  data points in the 22nd campaign were compared with the  $S_n$  based on the regression expression, as shown in Fig. 3. Here, the open gray circles indicate the data set obtained during the 19th and 21st campaigns, and the red open circle indicates the data obtained during the 22nd campaign. Note that there are some points deviating from the diagonal dashed line in the relatively low  $S_n$  region. The relatively large deviation was due to the limited number of parameters used

in the regression analysis. It was found that the newly obtained  $S_n$  in the 22nd campaign relatively well aligns with the diagonal line shown in Fig. 3, despite the regression expression being applicable only in the employed database range (gray points). However, it is indicated that this regression approach is applicable as a guideline to gradually extend the  $S_n$  range beyond the employed database.

Although the regression analysis suggests that the improvement of  $S_n$  is  $\sim 10\%$  during the 22nd campaign based on the maximum available NB injection power (Table 1), the actual improvement of  $S_n$  in the 22nd campaign experiment is  $\sim 20\%$ . The detailed investigation of this difference is our future work. There are two possible causes of this difference. The first is the additional heating source, ECH and ICH. In this regression analysis,  $P_{ECH}$  and  $P_{ICH}$  were excluded because of the relatively low importance of  $P_{ECH}$  in the preliminary regression analysis and no ICH in high  $S_n$  discharge performed during the 19th and 21st campaigns using a gas puff. The second is that the regression expression is merely guidance without any physics considerations. Despite the relatively high coefficient of determination, there was a dissociation of  $S_n$  identified by the regression analysis of experimental results. The improved regression expression can be deduced by including measurement data such as temperature, density, and neutron profiles, and so on. However, the current expression is better at the point of the feedback to the high  $S_n$  discharge scenario.

#### **4. Summary**

A trial for extending  $S_n$  record in steady-state discharge was performed in LHD based on a data-driven approach. The regression expression of  $S_n$  using externally controllable parameters was obtained using the  $S_n$  database established during the 19th and 21st LHD experimental campaigns. Data points were selected according to the general restriction of fulfilling high  $S_n$  discharge conditions. It was found that the injection power of N-NB was more important than the line averaged density and the injection power of P-NB. In the 22nd campaign, the high  $S_n$  record in steady-state discharge was successfully updated, based on the previously deduced regression expression. The new  $S_n$  record in steady-state discharge using a deuterium gas puff is  $3.7 \times 10^{15}$  n/s. Even though this regression expression is valid only within the range of the database, it is demonstrated to be effective as a plausible guideline for updating the  $S_n$  record gradually beyond the current database.

### **Acknowledgments**

This work is supported partly by the National Institute for Fusion Science Collaboration Research Program (KOA037), LHD project budgets (ULHH034), and JSPS KAKENHI Grant No. JP 19K03797.

### **References**

- [1] D. L. Jassby et al., Phys. Fluids B **3** (1991) 2308.
- [2] T. Nishitani et al., Nucl. Fusion **34** (1994) 1069.

- [3] F. X. Söldner et al., Nucl. Fusion **30** (1999) 407.
- [4] J. Karlsson and T. Elevant, Fusion Technol. **33** (1998) 341.
- [5] Y. Takeiri et al., IEEE Trans. Plasma Sci. **46** (2018) 1141.
- [6] A. Dinklage et al., Nature Physics **14** (2018) 855.
- [7] Y. Takeiri, IEEE Trans. Plasma Sci. **46** (2018) 2348.
- [8] M. Osakabe et al., Fusion Sci. Technol. **72** (2018) 199.
- [9] R. Seki et al., Plasma Fusion Res. **14** (2019) 3402126.
- [10] M. Isobe et al., Nucl. Fusion **58** (2018) 082004.
- [11] K. Ogawa et al., Nucl. Fusion **59** (2019) 076017.
- [12] K. Ogawa et al., Plasma Phys. Control. Fusion **60** (2018) 9.
- [13] K. Ogawa et al., Plasma Phys. Control. Fusion **60** (2018) 044005.
- [14] K. Ogawa et al., Nucl. Fusion **58** (2018) 044001.
- [15] K. Ogawa et al., Nucl. Fusion **58** (2018) 034002.
- [16] K. Ogawa et al., Plasma Fusion Res. **13** (2018) 3402068.
- [17] H. Nuga et al., Plasma Fusion Res. **14** (2019) 3402075.
- [18] K. Ogawa et al., Plasma Fusion Res. **14** (2019) 1202159.
- [19] H. Nuga et al., J. Plasma Phys. **86** (2020) 81586030.
- [20] S. Sangaroon et al., Rev. Sci. Technol. **91** (2020) 083505.

- [21] Y. Fujiwara et al., Nucl. Fusion **60** (2020) 112014.
- [22] S. Yamamoto et al., Nucl. Fusion **60** (2020) 068018.
- [23] K. Ogawa et al., Nucl. Fusion **60** (2020) 112011.
- [24] M. Isobe et al., IEEE Trans. Plasma Sci. **46** (2018) 2050.
- [25] K. Ogawa et al., Plasma Fusion Res. **16** (2021) 1102023.
- [26] K. Ogawa et al., Plasma Fusion Res. **15** (2020) 1202078.
- [27] M. Yokoyama and H. Yamaguchi, Nucl. Fusion **60** (2020) 106024.
- [28] M. Goto et al., Fusion Sci. Technol **58** (2010) 394.
- [29] M. Isobe et al., Rev. Sci. Instrum. **85** (2014) 11E114.
- [30] D. Ito et al., Plasma Fusion Res. **16** (2021) 1405018.
- [31] T. Akiyama et al., Fusion Sci. Technol **58** (2010) 352.
- [32] I. Yamada et al., Fusion Sci. Technol **58** (2010) 345.
- [33] K. Ikeda et al., Nucl. Fusion **59** (2019) 076009.

Table 1 Comparison of injection power during the 19th and 21st campaigns and the 22nd campaign in high  $S_n$  discharge. Here,  $P_{N-NB}$  and  $P_{P-NB}$  represent the injection power of the negative-ion-source-based neutral beam injector and the injection power of the positive-ion-source-based neutral beam injector, respectively.

Campaign	Maximum $P_{N-NB}$ (MW)	Maximum $P_{P-NB}$ (MW)
19th to 21st LHD campaigns	6.0	19.0
22nd LHD campaign	6.9	19.3

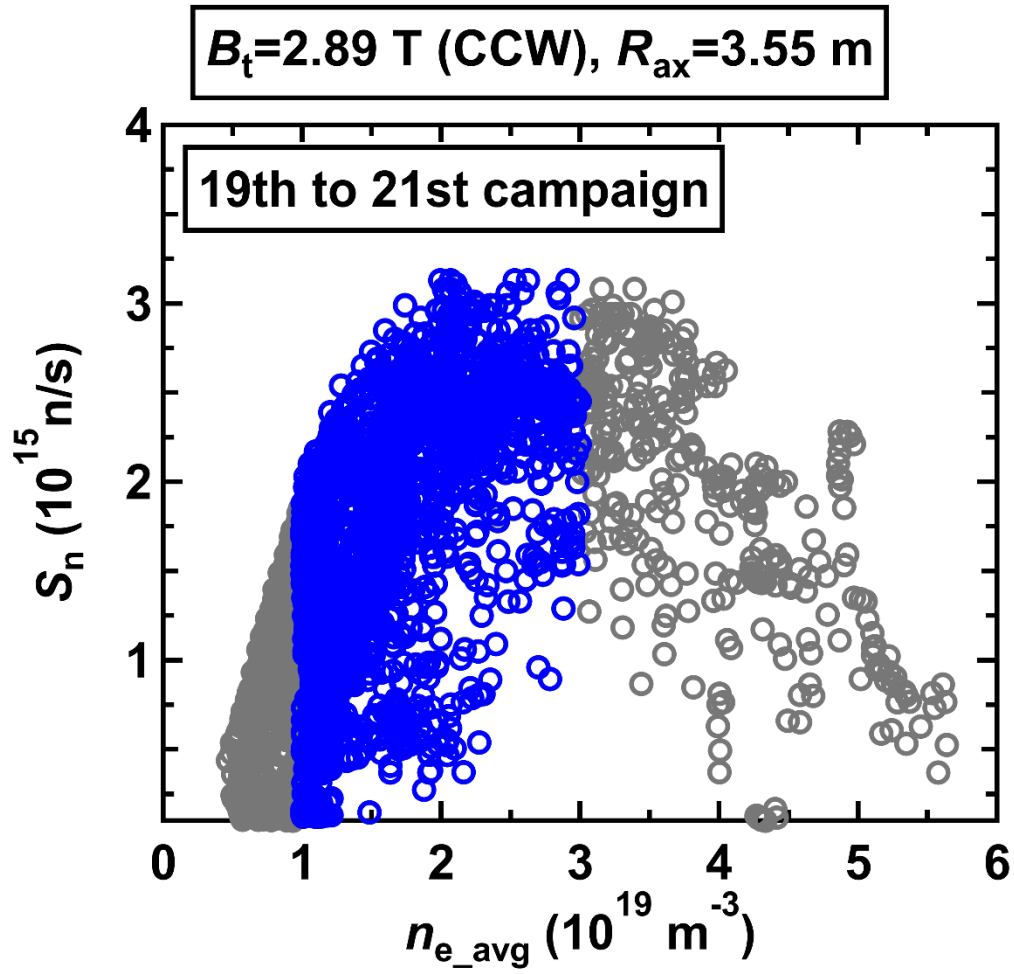


Figure 1. Total neutron emission rate ( $S_n$ ) as a function of the line-averaged electron density ( $n_{e\_avg}$ ) obtained in steady-state discharge using a deuterium gas puff during the 19th and 21st LHD campaigns at the toroidal magnetic field strength ( $B_t$ ) of 2.89 T with the counterclockwise (CCW) direction when viewing from the top and the magnetic axis position ( $R_{ax}$ ) of 3.55 m. Blue open circles correspond to the data points used for the regression analysis [13].

#163230,  $B_t=2.89$  T (CCW),  $R_{ax}=3.55$  m

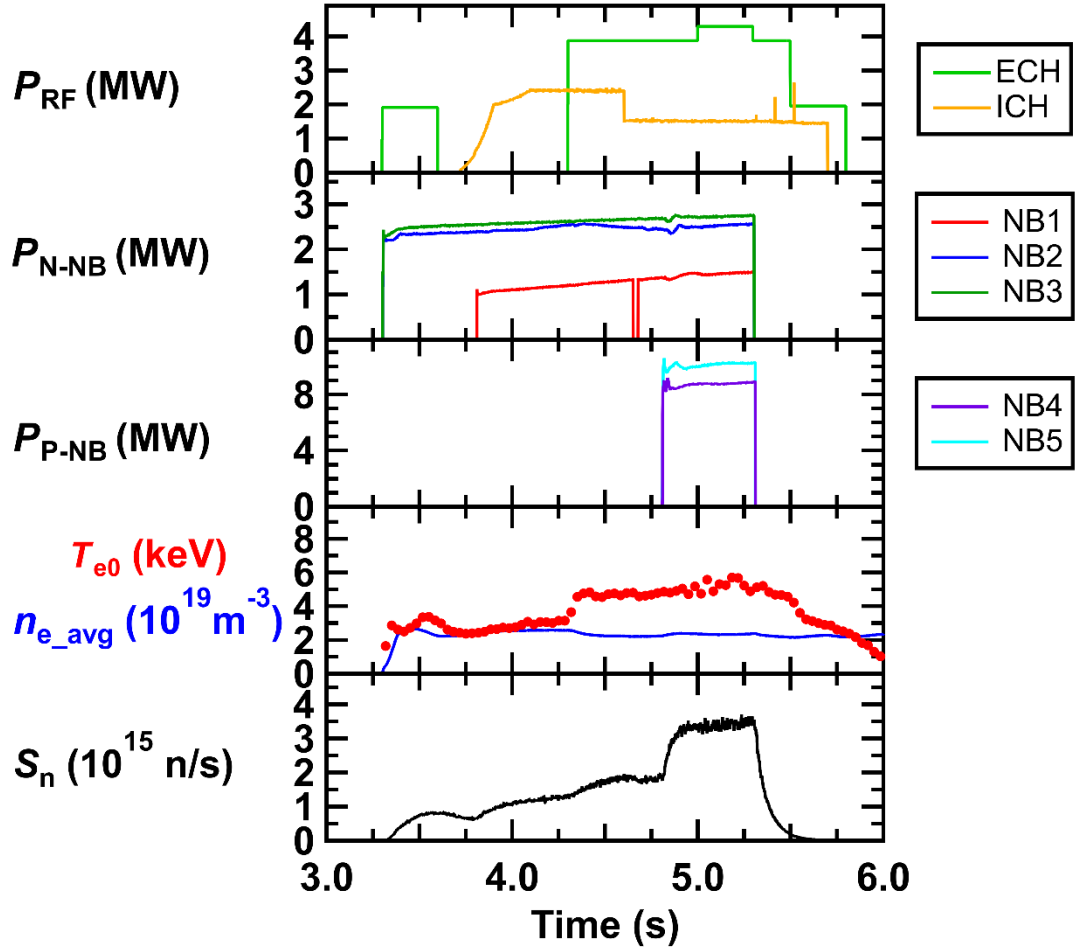


Figure 2. Maximum total neutron emission rate ( $S_n$ ) discharge using a deuterium gas puff in the 22nd campaign performed at the toroidal magnetic field strength ( $B_t$ ) of 2.89 T with the counterclockwise (CCW) direction when viewing from the top and the magnetic axis position ( $R_{ax}$ ) of 3.55 m. Here,  $P_{RF}$ ,  $P_{N-NB}$ ,  $P_{P-NB}$ ,  $T_{e0}$ ,  $n_{e\_avg}$ , ECH, ICH, and NB represent the injection power of the radiofrequency wave, the injection power of the negative-ion-source-based neutral beam injector, the injection power of the positive-ion-source-based neutral beam injector, the central electron temperature, the line-averaged

electron density, electron cyclotron heating, ion cyclotron range of frequency heating, and neutral beam injector, respectively. The obtained  $S_n$  record in steady-state deuterium discharge is  $3.7 \times 10^{15}$  n/s.

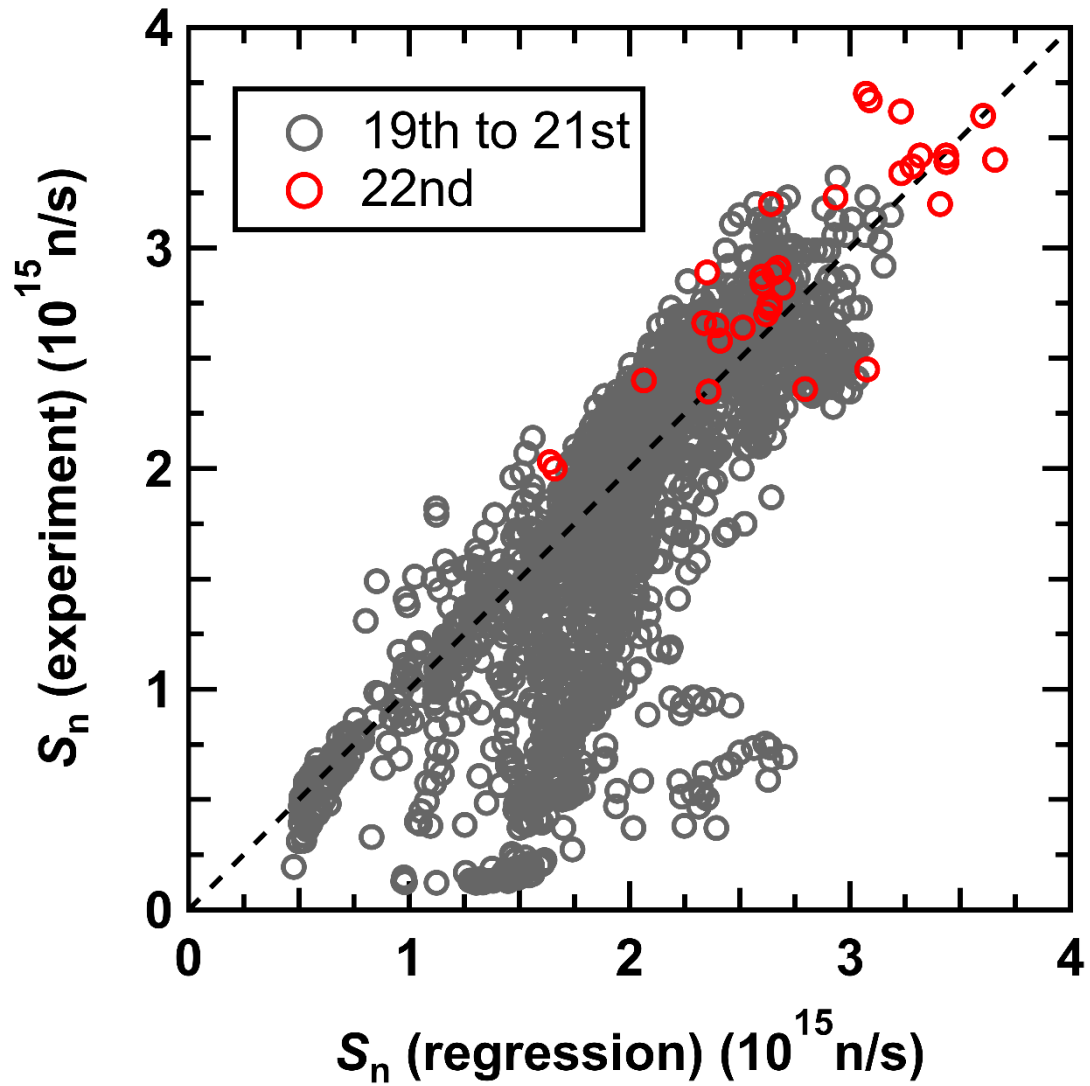


Figure 3. Comparison of experimentally obtained and calculated total neutron emission rate ( $S_n$ ) in steady-state discharges. Although the newly obtained data in the 22nd LHD experimental campaign (red circle) gradually increased beyond the database established during the 19th and 21st campaigns (gray circle), the data achieved almost align with the regression guidelines, as shown with a dashed line.